



THE UNIVERSITY *of* EDINBURGH

Edinburgh Research Explorer

Structural characterization and anti-inflammatory activity of two novel polysaccharides from the sea squirt, *Ascidiella aspersa*

Citation for published version:

Thomson, D, Panagos, CG, Venkatasamy, R, Moss, C, Robinson, J, Bavington, CD, Hogwood, J, Mulloy, B, Spina, D, Page, CP & Uhrin, D 2016, 'Structural characterization and anti-inflammatory activity of two novel polysaccharides from the sea squirt, *Ascidiella aspersa*' *Pulmonary Pharmacology and Therapeutics*, vol 40, pp. 69-79. DOI: 10.1016/j.pupt.2016.05.001

Digital Object Identifier (DOI):

[10.1016/j.pupt.2016.05.001](https://doi.org/10.1016/j.pupt.2016.05.001)

Link:

[Link to publication record in Edinburgh Research Explorer](#)

Document Version:

Peer reviewed version

Published In:

Pulmonary Pharmacology and Therapeutics

General rights

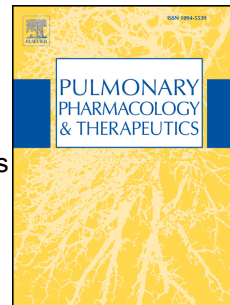
Copyright for the publications made accessible via the Edinburgh Research Explorer is retained by the author(s) and / or other copyright owners and it is a condition of accessing these publications that users recognise and abide by the legal requirements associated with these rights.

Take down policy

The University of Edinburgh has made every reasonable effort to ensure that Edinburgh Research Explorer content complies with UK legislation. If you believe that the public display of this file breaches copyright please contact openaccess@ed.ac.uk providing details, and we will remove access to the work immediately and investigate your claim.



Accepted Manuscript



Structural characterization and anti-inflammatory activity of two novel polysaccharides from the sea squirt, *ascadellia aspersa*

Derek Thomson, Claire Moss, Radhakrishnan Venkatasamy, Charalampos G. Panagos, Joanne Robinson, Charles D. Bavington, John Hogwood, Barbara Mulloy, Dušan Uhrín, Domenico Spina, Clive P. Page

PII: S1094-5539(16)30027-X

DOI: [10.1016/j.pupt.2016.05.001](https://doi.org/10.1016/j.pupt.2016.05.001)

Reference: YPUPT 1531

To appear in: *Pulmonary Pharmacology & Therapeutics*

Received Date: 21 March 2016

Revised Date: 10 May 2016

Accepted Date: 11 May 2016

Please cite this article as: Thomson D, Moss C, Venkatasamy R, Panagos CG, Robinson J, Bavington CD, Hogwood J, Mulloy B, Uhrín D, Spina D, Page CP, Structural characterization and anti-inflammatory activity of two novel polysaccharides from the sea squirt, *ascadellia aspersa*, *Pulmonary Pharmacology & Therapeutics* (2016), doi: 10.1016/j.pupt.2016.05.001.

This is a PDF file of an unedited manuscript that has been accepted for publication. As a service to our customers we are providing this early version of the manuscript. The manuscript will undergo copyediting, typesetting, and review of the resulting proof before it is published in its final form. Please note that during the production process errors may be discovered which could affect the content, and all legal disclaimers that apply to the journal pertain.

STRUCTURAL CHARACTERIZATION AND ANTI-INFLAMMATORY ACTIVITY OF TWO NOVEL POLYSACCHARIDES FROM THE SEA SQUIRT, ASCADELLIA ASPERSA

Derek Thomson², Claire Moss², Radhakrishnan Venkatasamy¹, Charalampos G. Panagos³, Joanne Robinson², Charles D. Bavington^{2†}, John Hogwood^{1,4}, Barbara Mulloy¹, Dušan Uhrín³, Domenico Spina^{1†}, and Clive P. Page^{1,5†}

From the ¹Sackler Institute of Pulmonary Pharmacology, Institute of Pharmaceutical Science, King's College London, SE1 9NH, United Kingdom; ²GlycoMar Ltd, European Centre for Marine Biotechnology, Oban, Scotland PA37 1QA; ³EaStCHEM School of Chemistry, Joseph Black Building, The King's Buildings, Edinburgh, EH9 3JJ, UK; ⁴National Institute for Biological Standards and Control, South Mimms, Herts, EN6 3QG

⁵To whom correspondence should be addressed: Sackler Institute of Pulmonary Pharmacology, Institute of Pharmaceutical Science, King's College London, SE1 9NH, United Kingdom. Tel: +44 207848 4784; E-mail, clive.page@kcl.ac.uk

[†]Joint senior co-authorship

Running title: *Novel anti-inflammatory polysaccharide substances*

Keywords: glycosaminoglycans / adhesion, elastase / inflammation / marine organisms

*This work was supported in part by grants from Veronapharma plc, and GlycoMar Limited to CPP and DS

The abbreviations used are: anti-IIa, anti-Xa, APTT, GAG, HCII, HPLC-SEC, HPLC, PDA, RI, FTIR, NMR, GC-FID, Gal, GalNAc, GalA, Glc, GlcA, GlcNAc, IdoA, Fuc

1. Introduction

There is considerable interest in the development of marine based molecules for the treatment of a variety of human conditions including pain, cancer [1, 2], thrombosis [3] and a range of inflammatory diseases [2, 4-7]. In the context of inflammatory diseases, the rationale for this development is the unequivocal demonstration that endogenous glycosaminoglycans (GAGs), like heparin, can modulate inflammatory responses *in vivo* [8]. In addition, these anti-inflammatory properties can be mimicked by non-anticoagulant species of heparin such as O-desulfated heparin [9, 10]. Heparin is a polysaccharide that acts via a wide range of anti-inflammatory mechanisms, which makes it a broad spectrum anti-inflammatory drug in addition to, and independent of, its anticoagulant activities [11]. The discovery of novel polysaccharides that share the anti-inflammatory actions of heparin, whilst lacking anticoagulant activity, provides the basis for the development of a novel class of anti-inflammatory drugs. The ability of heparin to bind to certain adhesion molecules that are integral to the inflammatory process, like P- and L-selectin, is to a large extent dependent on the protein surface charge distribution and the complementary sulfation pattern of the heparin [12, 13]. For example, heparin binding to P- and L-selectin prevents leukocyte adhesion to vascular endothelial cells, and hence, transmigration to inflammatory sites [2, 14]. Additionally, heparin shows other anti-inflammatory activities, the precise mechanism(s) of which are not yet fully understood [15].

The anti-inflammatory activity of heparin and related molecules has been tested in numerous clinical trials with some success [15], although to date only pentosan polysulfate is approved for the clinical treatment of an inflammatory

condition, interstitial cystitis [16], and as an intra-articular treatment for osteoarthritis in veterinary medicine. Nonetheless, there is increasing evidence supporting the use of heparin like molecules in the treatment of inflammatory conditions of the respiratory tract. For example, heparin has been shown to be effective in patients with chronic obstructive pulmonary disease (COPD) [17], asthma [18] and allergic rhinitis [19]. However, the anticoagulant properties of heparin limit the wider therapeutic utilisation of this drug in the treatment of inflammatory diseases, where anticoagulant activity is usually not desirable. Whilst the topical administration of heparin to mucosal surfaces in the respiratory tract is associated with limited systemic anticoagulant activity [20], the development of a non-anticoagulant molecule mimicking the anti-inflammatory effects of heparin would be preferable. Examples of this approach already exist and include a heparin-derived hypersulfated disaccharide that is effective against allergic inflammation in subjects with asthma [21].

Traditionally heparin is prepared from porcine and increasingly bovine sources. However, there are cultural sensitivities surrounding the use of porcine products in some communities and with the use of bovine-based material, a possibility of adverse effects exists, e.g. the occurrence of spongiform encephalopathy (BSE). Therefore a number of marine based polysaccharides has been evaluated for their anti-inflammatory activity [6, 22], as these eliminate the challenges and risks associated with molecules sourced from mammals [23]. One of the polysaccharides that has often been extracted from marine sources is dermatan sulfate, another member of the GAG family that has been shown to have anti-inflammatory properties, as well as being shown to participate in cell growth, differentiation and morphogenesis, cell migration and infections from bacteria and viruses [24]. Mammalian dermatan sulfate has been suggested as a potential alternative to heparin as it exhibits lower

anticoagulant activity than heparin and therefore its use poses a smaller risk of hemorrhage [25]. Dermatan sulfates with a variety of degrees and patterns of sulfation have been identified in the past in Ascidians, but some of these polysaccharides have been shown to also have anticoagulant activities [26, 27].

Chitin is an unsulfated marine derived polysaccharide, one of the most abundant polysaccharides on earth, and the most abundant renewable polymer in the oceans. It is a linear polysaccharide consisting of β -1,4-*N*-acetyl-D-glucosamine monosaccharide units. The main role of chitin is to participate in the construction of protective tissues like the exoskeleton of arthropods, e.g. shrimps and lobsters, as well as the cell walls of fungi and the exoskeleton of insects [28]. However, chitin can also participate in the formation of signalling molecules, for example the lipochitin oligosaccharides that are produced by rhizobia [29]. The fucosylation of the C6 of the reducing end *N*-acetylglucosamine by the NodZ chitin oligosaccharide fucosyltransferase has been shown to extend the range of hosts for certain bacteria [30]. Aberrant fucosylation of the GlcNAc moieties of glycoproteins has been reported in several types of cancer [31]. In general, the fucosylation of various glycoproteins has been observed in a multitude of different organisms, from insects to animals [32, 33], and has been suggested to be responsible for the regulation of various biological activities [34, 35].

Here we present the structural analysis and pharmacological properties of two novel polysaccharides (VRP327A & B) isolated from the ascidian (more commonly named sea squirts) *Ascidella aspersa*

2. Materials and methods

2.1 Materials

Ethylenediaminetetraacetic acid (EDTA) and trimethylsilyl propionate (TSP) were purchased from Goss Scientific Instruments Ltd and Aldrich respectively. The sea squirt *Ascidiella aspersa* was obtained from Loch Fyne Seafarms (Tarbert, Loch Fyne, Scotland), where the tunic was removed and discarded, and the remainder of the animal stored frozen (-20 °C).

Fucoidan from *F. vesiculosus* was obtained from Glycomix Ltd, Reading, UK.

2.2 Extraction of Polysaccharides from sea squirts

Extracts were prepared by digestion of approximately 20 kg of homogenized tissue with alcalase (5 ml/kg wet weight, Novozymes) for 16 h at 60 °C, pH 8.0 with continuous stirring. The polysaccharides were recovered from the strained liquor by mixing with pre-equilibrated anion exchange resin (1:1 mixture of Lewatit VPOC1074 and S6328A, Caldic, UK), 200 g / kg marine tissue. The eluted product was then cleaned-up by further size-exclusion (Sephacryl S100, GE) and ion exchange (Q Sepharose FF, GE) chromatography. The final product was dried by lyophilisation or spray drying.

2.3 Free radical depolymerisation of polysaccharide B

The polysaccharide sample was in some cases subjected to free radical depolymerisation based on the method of Volpi [36]. The polysaccharide (60 mg) was

dissolved in water (25 ml) and the solution was brought to 50 °C following addition of Copper (II) acetate (monohydrate) (50 mg). The pH was adjusted to a value between 7.5 and 8 using NaOH. The depolymerisation was then initiated by continuous addition (using syringe pumps) of hydrogen peroxide and sodium hydroxide, with flow rates adjusted to maintain pH 7 – 8. On completion of the depolymerisation, the reaction was stopped by adding 20 % acetic acid and Chelex. The final solution was cleaned-up by preparative chromatography on Q-Sepharose to remove the Copper, and fractionated on sephacryl S30 before lyophilisation.

2.4 Molecular weight determination

The molecular weight (MW) of finished products was determined by high performance liquid chromatography (HPLC), size exclusion chromatography (SEC) with refractive index (RI) and/or photodiode array detection (PDA). Samples were analysed using both a Biosep SEC 4K column (300 x 7.80 mm, Phenomenex), which has a higher molecular weight range (determined as 12 kDa to 670 kDa), and if necessary a YMC Diol 120 (250 x 4.6 mm, YMC Europe) column which has a lower molecular weight range (determined as 1,340 Da to 8,040Da). Both columns were calibrated with standard dextrans (Fluka) run under the same conditions. Samples were prepared at 1 mg/ml in the mobile phase (1 mM EDTA, 0.9 % NaCl, 50 mM Tris, pH 7.0) and 20 µl injections were analysed over 15 min using a Waters 2695 HPLC system running at 1 ml/min with a column temperature of 30 °C. Data were collected by RI and PDA (190-400 nm).

2.5 Uronic acid determination

The uronic acid content was determined after acid hydrolysis (6.0 M HCl at 100 °C for 6 h) by the modified carbazole reaction as previously described [37].

2.6 Protein Content determination

Protein content was determined using a Pierce 660 nm protein assay (Thermo) in accordance with manufacturer's instructions. Calibration curves were constructed using bovine serum albumin (Sigma) standard solutions.

2.7 Sulfate Assay

We used a previously described technique for the determination of small amounts of sulfate present in GAGs [38]. To minimise the amounts required of each valuable sample, the method was miniaturised for use in a microplate format. Samples were hydrolysed by mixing a 1 mg/ml solution in water (25 µl) with an equal volume of 1 N HCl and heating for 1-2 h at 100 °C. The hydrolysed samples were dried in a vacuum centrifuge at 60-65 °C. The dried hydrolysate was reconstituted in deionised water (250 µl). Matching, non-hydrolysed samples were run alongside the hydrolysed samples, at a concentration of 1 mg/ml. Sulfate content was determined by mixing each sample (100 µl) with ethanol (400 µl) in a microfuge tube and this mixture (125 µl) was then added to a 96-well microplate. BaCl₂ buffer (50 µl) was then added to each well followed by sodium rhodizonate solution (75 µl). The microplate was shaken for 30 sec on a plate shaker and then incubated in the dark at room

temperature for 10 min, followed by a further 30 sec shake and final measurement of colour intensity using a plate reader set to 520 nm.

2.8 Disaccharide Analysis

The disaccharide composition of the polysaccharide was determined by HPLC using an established [39]. Samples were digested at a final concentration of 5 mg/ml in digest buffer (0.5 mM Tris 0.01 mg/ml BSA 5mM NaCl pH 7.0) with 1.4 mU of heparinase II (Grampian Enzymes) or 2.5 mU of chondroitinase ABC (Grampian Enzymes), overnight at 25 °C. Samples were analysed with and without hydrolysis in order to identify free disaccharides which might lead to misinterpretation of the disaccharide composition. Heparin (Acros) and shark chondroitin sulfate (Sigma) were used as control enzyme substrates. The digested samples were analysed by HPLC strong anion exchange chromatography using a ProPac PA1 Analytical column (4 x 250 mm, Dionex) and a Waters 2695 separation system equipped with a PDA detector. Standard heparin and chondroitin disaccharides (Dextra Labs) were used for calibration purposes. The digested samples and controls were loaded (20 µl) and eluted with a salt gradient (buffer A, dH₂O pH 3.5) rising to 60 % buffer B (2M NaCl pH 3.5) after 30 min, monitoring at 232 nm.

2.9 Monosaccharide analysis

The monosaccharide composition of samples was determined by methanolysis / TMS derivatisation followed by gas chromatography with flame ionisation detection. The

sample (0.1 mg) was mixed with scyllo-inositol internal standard (5 nmol) and was treated with 100 μ l 0.5 M methanolic HCl in an oven-treated sealed glass reacti-vial for 4 h at 85 °C. After cooling, neat pyridine (20 μ l) was added to neutralize the HCl, mixed, and neat acetic anhydride (20 μ l) was added to re-N-acetylate any free primary amines. The samples were dried overnight in a vacuum centrifuge, followed by addition of methanol (40 μ l), after which they were dried again for 2 h. Samples were reacted with Tri-methylsilane reagent (TMS, 40 μ l, Supelco) in sealed reacti-vials for 10 min. Samples were analysed by GC-FID: 1 μ l injections were analysed on a Shimadzu GC-2014 machine with FID using a ZB5-ms column (30 m x 0.25 mm id x 0.25 μ m film thickness) at 300 °C. Monosaccharide standards were prepared and analysed in the same way: arabinose (A3131 Sigma) xylose (X-1500 Sigma), mannose (M6020 Sigma), fucose (F2252 Sigma), rhamnose (R3875 Sigma), galactose (G0750 Sigma), glucose, glucosamine (G4875), galactosamine (G0500), glucuronic acid (G5269), galacturonic (48280 Fluka) and sialic acid were all prepared as 100 mM stock solutions. Monosaccharide composition of samples was determined on the basis of peak areas with a response factor calculated from the peak area for each monosaccharide standard relative to the internal control.

2.10 FTIR spectroscopy

Transmission FTIR spectra were collected for selected samples and reference compounds (chitin, dermatan sulfate and chondroitin sulfate B, all obtained from Sigma) prepared in potassium bromide tablets. Transmittance data were analysed using Essential FTIR software.

2.11 Cell viability

HeLa cells were grown under standard tissue culture conditions (37 °C, 5% CO₂), until a 90 % confluent monolayer was achieved. The cells were then trypsinized, transferred into a tube and centrifuged (200 g) to form a pellet, and re-suspended in growth media and then added to a microplate (4 x 10³ cells/well; 100 µL). Cells were incubated in the absence or presence of sea squirt polysaccharides for a period of 24 h at 37 °C, 5 % CO₂. XTT labelling reagent and electron-coupling reagent from the cell proliferation kit (Cell Proliferation kit II (XTT), Roche) was added to the wells (50 µL) for a period of 4 h at 37 °C, 5 % CO₂. Absorbance was measured at 492 nm with a reference wavelength of 690 nm. The percentage viability of cells was expressed as the absorbance of test agents as a percentage of control values.

2.12 Anticoagulant activity

Characterization of the anticoagulant activity (anti-factor IIa, anti-factor Xa, activated partial thromboplastin time (APTT) and heparin cofactor II (HCII) assays) of the sea squirt samples was performed using a previously published protocol [40].

2.14 Pre-kallikrein activation assay

In order to investigate the interaction of the sea squirt polysaccharides with the contact activation pathway, a pre-kallikrein activation assay was carried out as previously described [40]. Briefly, a dilution series of the samples and a dextran sulfate (*Leuconostoc mesenteroides*, Sigma) positive control were set up, and each of the seven concentrations was mixed with normal pooled plasma (George King Bio-

Medical Inc.) as described elsewhere [41]. After a 5-min activation period at 37 °C, a chromogenic substrate specific for plasma kallikrein was added (Chromogenix S2302), and color development, indicating substrate cleavage, was measured after 4 min (A405–490 nm). The change in absorbance was compared with a blank control related to the amount of kallikrein in the blood resulting from pre-kallikrein activation by test samples. Four runs were carried out, and a concentration-response curve was generated for each sample.

2.15 Elastase release from human neutrophils

Human neutrophils were isolated from whole blood isolated from the antecubital vein of healthy volunteers using citrate as an anticoagulant. Ethics permission was obtained from National Research Ethics Service – North of Scotland, for these experiments. Neutrophils were isolated using a previously described technique [42–46], washed and suspended in HBSS (PAA) at a final concentration of 2.5×10^6 cells/ml. This cell suspension (150 μ l) was added to microtubes containing HBSS (22 μ l; PAA), cytochalasin B (25 μ l, 40 μ g/ml; Sigma) and TNF α (25 μ l 80 ng/ml; Merck) to give a final concentration of 5 μ g/ml and 10 ng/ml, respectively for 30 min at 37 °C in the absence or presence of increasing concentrations of a novel marine polysaccharide. The formyl peptide ligand, f-met-leu-phe (fMLP)(25 μ l, 100 ng/ml; Sigma) was then added and cells incubated for a further 45 min at 37 °C. The microtubes were then centrifuged (5000 rpm; 2000g) for 5 min to pellet the cells and the supernatant (25 μ l) added in triplicate to a 96-well microplate for the determination of measurement of elastase release. In brief, Tris buffer (150 μ l, 0.1M) and neutrophil elastase substrate 1 (MeOSuc-Ala-Ala-Pro-Val-pNA; 20 μ l, 0.5 mg/ml; Merck) were

added to each well and absorbance measured at 405 nm every 5 min for 1 h and V_{max} calculated over 4 data points between 10 min and 1 h. Data are expressed as percentage of control samples.

2.16 Neutrophil adhesion assay

Human umbilical vein endothelial cells (HUVEC) (Promocell) were cultured in accordance with the supplier's instructions and grown to confluence in flat-bottomed 96-well cell culture plates. Human neutrophils were isolated from fresh whole blood obtained from the antecubital vein of male healthy volunteers as described above and stained with Calcein AM (Invitrogen) by adding the Calcein AM (12.5 μ l, 1 mg/ml stock) in DMSO to 3.6×10^7 cells (5 ml) to give a final concentration of 2.5 μ M. The cells were incubated at 37 °C, 5 % CO₂ for 30 min and centrifuged at 400 g for 10 min. The resulting cell pellet was washed 2-3 times by re-suspending in HBSS (5-10ml) followed by centrifugation. After the final wash, cells were re-suspended into HBSS at a density of 1×10^6 cells/ml. HUVECs were stimulated prior to addition of labelled neutrophils by the addition of 10 Uml⁻¹ IL-1 β and TNF α , followed by a 6 h incubation at 37 °C, 5 % CO₂. The HUVECS were then washed with HBSS followed by addition of 2×10^5 labelled neutrophils to each assay well. Three test plates were run in parallel: unstimulated HUVECs with no test compounds, stimulated HUVECs with no test compounds, and stimulated HUVECs with test compounds added. The plates were incubated for 15 min at 37⁰C in 5% CO₂ after which non-adherent cells were removed by washing 2-3 times with assay buffer. The plates were then read by measuring fluorescence using 485/530 nm excitation/emission filter sets on a Biotek Synergy 2 plate reader. Data were expressed as percentage adhesion relative to controls.

2.17 Neutrophil migration assay

HUVECs (Promocell) were cultured in accordance with the supplier's instructions and grown to confluence in tissue culture flasks. The endothelial cells were released from the culture flasks by trypsinisation (HUVEC Detach Kit, Promocell), and re-suspended in pre-warmed endothelial growth medium at a concentration of 3×10^5 cells/ml. A HUVEC suspension (100 μ l) was added above the transwell filter (24-well Thincert Plates, Greiner) of each well in the plate and media (600 μ l) below the filter and incubated at 37 °C, 5 % (V/V) CO₂, until a confluent monolayer of cells was formed. Neutrophils were isolated from fresh whole donor blood and stained with calcein AM as described above. The HUVECs were stimulated by adding to each well IL-1 β (11 μ l of 0.2 μ g/ml) and TNF α (11 μ l of 0.2 μ g/ml) to achieve final working concentrations of 0.01 μ g/ml IL-1 β and TNF α . The wells were treated with HBSS (22 μ l) and all wells were incubated for 6 h at 37 °C, 5 % (V/V) CO₂. On completion the transwell filters were transferred to an empty 24 well plate. The media from below the well was removed and rinsed out once with HBSS, before adding fresh HBSS (600 μ l) to the lower chamber. The media from above the filter was gently removed and the HUVECs washed carefully using HBSS (200 μ l). The filters were returned to the original 24 well plate containing the fresh HBSS and 22 μ l of 10X the test compound was added shortly thereafter, followed by stained neutrophils (100 μ l) into the top chamber, bringing the volume up to 222 μ l. IL-8 was used as the chemoattractant, by adding IL-8 (60 μ l of 1 mg/ml stock) to the lower chamber, and HBSS (60 μ l) to the lower chamber in all other groups. In a separate 24 well plate, labelled neutrophils

(100 μ l) were added to HBSS (600 μ l). The plates were then incubated for 90 min at 37 °C in 5 % CO₂ to allow cells to migrate. In order to remove test cells with non-specific binding from above the filter, the media and cells from above the filter were transferred to a 96 well solid black plate. Each filter was gently washed twice with HBSS (200 μ l) and transferred to the black 96 well plate. The fluorescence from this fraction is referred to as the non-adherent component. The filters were transferred to a solid black 24 well plate to be read, with this being referred to as the adherent component. The media in the lower chamber was transferred into a solid black 96 well plate and the well was rinsed with HBSS, which was also then transferred to the 96-well black plate. The fluorescent reading from this fraction is referred to as the migrated component. All readings were blanked by reading wells containing HBSS only and the filter readings were blanked with a clean wet filter. The media from the well on the separate control 24 well plate containing the neutrophils was transferred to a solid black 96 well plate and read to provide a control for the total fluorescent value of labelled cells. Fluorescence was read as described above.

2.18 *In vivo* peritoneal inflammation model

Male BALBc mice (6 -8 weeks; 20-22 g) were obtained from King's College London and maintained on a 12 h light/12 h dark cycle, and were allowed food and water *ad libitum*. Animals were housed in standard caging (5 mice per cage) with appropriate bedding and enrichment. All of the experiments undertaken within this study were

approved under the Animals [Scientific Procedures] Act (1986) and carried out in accordance with the ARRIVE guidelines.

We utilized a modification of our previously published method to assess neutrophil recruitment to the peritoneal cavity of mice [47] to investigate the effect of the sea squirt polysaccharides. Mice were randomized to receive an intravenous injection of either saline control or test substance. After 15 min of vehicle or test substance, zymosan A (0.5 ml; Sigma Chemical) was injected intraperitoneally to give a total dose of 1 mg/mouse. Four hours later, mice were killed by an overdose of CO₂ and 3ml of saline was injected into the peritoneal cavity. The peritoneal cavity of each mouse was then massaged for 1 min and a small incision made to the lower abdomen to reveal the peritoneal cavity, and lavage fluid (2ml) was collected and stored on ice. Total and differential cells counts were enumerated. A dose response relationship was undertaken to assess the *in vivo* potency of these molecules as anti-inflammatory agents *in vivo*.

2.19 Statistical Analysis

Statistical analysis was performed using Graphpad prism (Graphpad, version 5). The null hypothesis was tested using analysis of variance for grouped data and an appropriate post-hoc test was applied; the mean values were considered significantly different when $p < 0.05$. In other instances, dose response data were fitted to a 3 parameter logistic equation to determine potency. Data are expressed as mean \pm sem.

2.20 NMR analysis

All lyophilized samples were dissolved in 100 % D₂O (540 µl) containing deuterated NaH₂PO₄+HNa₂HPO₄ buffer (10 mM, pH 7.2). A stock solution of EDTA and TSP (20 µl) was then added. The stock solution was prepared by dissolving EDTA (4 mg) and TSP (9 mg) in the phosphate buffer (200 µl). The pH was adjusted to 7.2 by adding a few drops of a concentrated solution of NaOH in D₂O. All spectra were acquired at 50 °C on an 800 MHz Avance I (Bruker) NMR spectrometer equipped with a z- gradient triple-resonance TCI cryoprobe. The spectra were referenced using ¹H and ¹³C signals (0 ppm) of TSP.

1D ¹³C NMR spectra were acquired using relaxation and acquisition times of 1.5 and 0.185 s; 40960 scans were accumulated in 20 h per spectrum. FIDs were zero filled once and a 2 Hz exponential line broadening was applied prior to Fourier transformation. 2D ¹H, ¹³C HSQC spectra were acquired using *t*₁ and *t*₂ acquisition times of 22 and 106 ms, respectively; 10 scans were acquired into each of 800 *F*₁ complex data points resulting in the total experimental times of 3.5 h per sample. The standard 2D ¹H, ¹³C HSQC-TOCSY BRUKER pulse sequence was modified by appending a ¹H spin-echo of overall duration of 1/¹*J*_{CH} (optimized for a ¹*J*_{CH}=150 Hz) after the TOCSY spin-lock and two 2D ¹H, ¹³C HSQC-TOCSY spectra were acquired in an interleaved manner. The first with, and the second without, an 180° ¹³C pulse applied simultaneously with the 180° ¹H pulse of the final spin-echo. This resulted in a change of the sign of one-bond cross peaks between the two spectra. Addition of the two 2D matrices prior to processing yielded a 2D ¹H, ¹³C HSQC-TOCSY spectrum with substantially reduced one-bond cross peaks. Such treatment has facilitated identification of weak TOCSY cross peaks. The subtraction of the two original spectra yielded a ¹H, ¹³C HSQC spectrum. Each 2D ¹H, ¹³C HSQC-TOCSY spectrum

was acquired using t_1 and t_2 acquisition times of 44 and 106 ms, respectively; 1600 complex data points using 24 scans were collected in F_1 in each experiment; the total duration of the experiment was 18 h. Spin-lock was achieved via DIPSI-2 mixing sequence applied for 25 or 60 ms. 2D ^1H , ^{13}C HSQC-NOESY spectra for the polysaccharides were acquired using t_1 and t_2 acquisition times of 21 and 106 ms; 750 complex data points were collected in F_1 using 192 scans; the total duration of the experiment was 66 h. The NOESY mixing time was 25 ms. 2D ^1H , ^{13}C HMBC spectra for the VRP 327B oligosaccharides were acquired using t_1 and t_2 acquisition times of 14 and 367 ms; 1024 complex data points were collected in F_1 ; the total duration of the experiment was 8.5 h. The experiment was optimized for the $^nJ_{CH}$ of 6 Hz and a two-stage one-bond correlation filter was set for $^1J_{CH}$ of 120 (minimum) and 160 (maximum) Hz.

3. Results and discussion

3.1 Monosaccharide analysis of the sea squirt samples.

The initial sea squirt samples analysed contained a mixture of polysaccharide A and B (43% of A and 48% B polysaccharides, respectively which we have designated as VRP327A and VRP327B) (Table 1). Due to size and charge similarities between polysaccharide A and B it was not possible to separate them fully. Nevertheless, NMR was able to guide the HPLC purification process, resulting in two samples, one of them containing 83% polysaccharide A and 13% B, with another one containing 20% polysaccharide A and 73% B.

Table 1: Monosaccharide analysis of three sea squirt samples

Monosaccharide	Polysaccharide rich sample A	Polysaccharide rich sample B	Initial sample
Arabinose	0	0	0
Rhamnose	0	3.45	2.58
Fucose	4.28	25.16	18.71
Xylose	0.8	0.84	1.3
IdoA	40.92	9.85	24.5
Mannose	0	0.42	1.22
Galactose	2.54	1.67	2.72
Glucose	0.55	0.48	0.68
GlcA	1.61	1.28	1.91
GalNAc	40.9	8.54	16.91
GlcNAc	8.4	48.31	29.47

Both polysaccharides A and B had molecular weights > 100 kDa. In the initial monosaccharide analyses we performed, it was not possible to distinguish IdoA, which is found in DS, from GlcA, which is found in CS, due to lack of availability of appropriate IdoA standards. However, in the last 2 batches analysed, it was possible to distinguish between the two, and it was confirmed that IdoA was the main uronic acid present in polysaccharide A. The main distinguishing feature of polysaccharide B with A was the presence of higher levels of fucose ($>20\%$) and N-acetyl glucosamine ($>35\%$) in B. A number of samples with mixed composition were analysed, giving intermediate monosaccharide composition.

3.2 FTIR spectroscopy

The FTIR spectrum of a sample of *A. aspersa* polysaccharide A in a KBr tablet is shown in Figure 1, overlaid with spectra from chitin and dermatan sulfate, for comparison. The spectrum is indicative of the structural features of a GAG like molecule. The peaks at 1259 cm^{-1} and 821 cm^{-1} are sulfate vibrations, multiple broad peaks around 1054 cm^{-1} are sugar ring vibrations, and the peak at 1637 cm^{-1} may combine amide vibration arising from hexosamines and C=O vibration of uronic acids. No attempt was made to distinguish between polysaccharides A & B by FTIR,

but the date shown confirms the similarity between polysaccharide A and dermatan sulfate, and major differences from chitin.

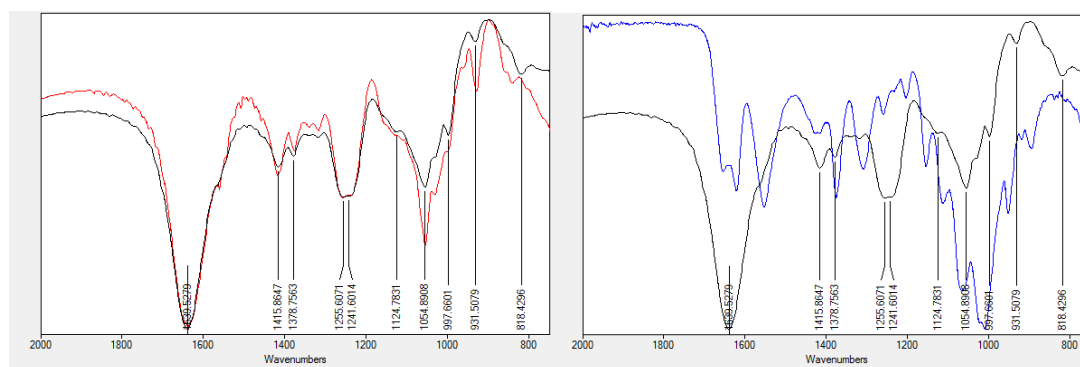


Figure 1: (A) FTIR spectrum of Polysaccharide A (black) overlaid on the spectrum (red) of reference dermatan sulfate (Sigma), (B) Polysaccharide A (black) overlaid on the spectrum (blue) of reference chitin (Sigma), all in KBr tablet. Spectrum shows absorbance plotted against wavenumber with absorbance maxima shown in black text for polysaccharide A

3.3 NMR analysis of polysaccharide A (VRP327A)

The monosaccharide analysis suggested that polysaccharide A is a dermatan sulfate. Initial 1D ^1H and ^{13}C spectra showed that the sample was too complex and full resonance assignment was therefore obtained using 2D ^1H , ^{13}C HSQC and 2D ^1H , ^{13}C HSQC-TOCSY spectra. The 2D ^1H , ^{13}C HSQC-NOESY spectrum helped to verify the assignment and also provided information about the nature of glycosidic bonds. The results showed that polysaccharide A consists mainly of a highly sulfated disaccharide repeating unit $\rightarrow 4)\text{IdoA}(1\beta\rightarrow 3)\text{GalNAc } 4,6\text{SO}_4(1\beta\rightarrow$. In addition, GalNAc4SO₃ and GalNAc6SO₃ monosaccharides and a small amount of GlcA were identified in agreement with the monosaccharide analysis. The chemical shift comparison with similar polysaccharides showed a very good agreement with all identified disaccharide structural motifs in polysaccharide A (Table 4).

Table 2. $^1\text{H}/^{13}\text{C}$ chemical shifts of polysaccharide A.

	GalNAc4,6SO ₄	GalNAc4SO ₄	GalNAc6SO ₄	IdoA	GlcA

H1/C1	4.69/105.22	4.62/105.23	4.72/104.29	4.89/106.00	4.51/107.0
H2/C2	4.06/54.64	4.06/54.05	3.99/53.89	3.56/72.12	3.37/75.32
H3/C3	4.05/ 78.18	4.10/78.41	3.82/83.13	3.96/73.96	3.59/76.82
H4/C4	4.71/ 78.71	4.70/78.60	N.D.	4.08/84.07	3.75/84.52
H5/C5	4.10/ 75.2	4.10/ 75.2	3.96/75.48	4.72/72.35	3.7/79.23
H6/C6	4.22/ 70.65	3.78/63.88	4.22/70.27	-/176.6	-/176.73
NAc	2.09/25.5	2.04/25.4	2.06/25.7	-	-

N.D. Not detected

^1H and ^{13}C resonance assignment obtained for polysaccharide A are in a good agreement with the literature data; namely, the assignment of the GalNAc4,6SO₄ was corroborated by the comparison with the corresponding data for the 4,6 sulfated CS[48]; the values for GalNAc4SO₄ agreed with the mammalian DS data [49] and GalNAc6SO₄ were in agreement with the Ascidian DS data[27]. The assignment of the IdoA was corroborated by the comparison with the corresponding data reported for a mammalian DS [49], while the GlcA data agreed with the porcine DS [50] and CS oligosaccharide data [51].

Integration of the C2 and C6 cross peaks of GalNAc4S, GalNAc6S and GalNAc4,6S in 2D ^1H , ^{13}C HSQC spectrum of polysaccharides A indicates that GalNAc4,6S constitutes approximately 75% of the total GalNAc content, whereas GalNAc4S and GalNAc6S constitutes the remaining 25%, approximately at 1:1 ratio. The integration of the anomeric carbons of GlcA and IdoA showed that IdoA constitutes 80% of the total uronic acid content, while GlcA is only present at the 20%.

3.4 NMR analysis of polysaccharide B (VRP327B)

The monosaccharide analysis of polysaccharide B indicated that its main components are N-acetylated glucosamine and fucose (2:1 ratio, Table 1). This is in agreement with the NMR results. Here H2/C2 resonances at 3.71-3.77/58.69-59.03 ppm confirmed the presence of GlcNAc, as opposed to GlcNH₂ for which H2 is

typically observed at about 0.8 ppm lower chemical shift [52]. In addition, the $^1\text{H}/^{13}\text{C}$ signals of the N-acetyl group were present at 2.04-2.16/23.25-25.49 ppm. Uninterrupted sequential transfer of magnetization from H1 to H6 seen in the 2D ^1H , ^{13}C HSQC-TOCSY spectrum of polysaccharide B is a consequence of axial-axial arrangement of protons in GlcNAc. The analysis of 2D ^1H , ^{13}C HSQC-TOCSY spectrum identified four distinct sets of GlcNAc resonances (M1-M4 in Table 3), indicating structural heterogeneity of this polysaccharide.

Table 2: $^1\text{H}/^{13}\text{C}$ chemical shifts of four different GlcNAc residues and fucose residues identified for polysaccharide B. GlcNAc molecules M1 and M2 are branched with C3-sulfated fucose on C4, while GlcNAc M3 and M4 are sulfated at C4. M2 is also sulfated at C6.

	GlcNAc (M1)	GlcNAc (M2)	GlcNAc (M3)	GlcNAc (M4)	Fucose
H1/C1	4.54/103.32	4.62/103.04	4.76/102.42	4.72/102.67	5.04/101.34 4.92/101.56
H2/C2	3.72/58.97	3.74/58.71	3.77/58.69	3.71/59.03	3.93/68.71
H3/C3	4.10/78.08	4.13/78.15	4.17/80.05	4.14/79.82	4.49/80.47
H4/C4	3.72/76.30	3.76/76.88	4.08/78.42	4.00/78.83	4.13/73.03
H5/C5	3.43/77.48	3.68/75.59	3.70/78.28	3.60/77.46	4.75/69.29
H6/C6	3.91/62.70	4.33-4.55/ 65.84	3.76-3.96/ 64.93	3.75-4.03/ 64.58	1.29/18.48

With regard to fucose, the H6/C6 resonances at 1.29/18.48 ppm confirmed the presence of this residue in polysaccharide B. Unlike in GlcNAc, only one set of fucose cross peaks were seen for H2/C2 to H6/C6 pairs, while two sets of resolved H1/C1 cross peaks were attributed to fucose. Comparison of ^1H and ^{13}C chemical shifts of fucose in polysaccharide B with those in fucosylated chondroitin sulfate (fCS) [40] showed that fucose of polysaccharide B is sulfated at position C3.

The 2D ^1H , ^{13}C HSQC-NOESY spectrum of polysaccharide B contains intra- and inter-residue H1-H3 cross-peaks indicating the existence of $\rightarrow 3)\text{GlcNAc}(1\beta\rightarrow 3)\text{GlcNAc}(1\beta\rightarrow$ linkages. NOE cross peaks between H4 of

GlcNAc and H1 of fucose identified in the 2D ^1H , ^{13}C HSQC-NOESY spectrum, as well as the inter residue HMBC cross peak between C4 of GlcNAc and H1 of fucose, showed that the M1 and M2 GlcNAc residues are branched by fucose at C4 positions. The M1/M2 chemical shifts differ significantly only for H5/C5 and H6/C6 pairs; in particular the H6/C6 atoms have higher chemical shift in M2 than in M1. This increase is consistent with C6 sulfation of M1/M2 GlcNAc residues.

The ^1H and ^{13}C chemical shifts of corresponding atoms in M3 and M4 are very similar and their H4/C4 chemical shifts are higher than seen for M1/M2, indicating that in M3/M4 these positions are sulfated. A comparison with the chemical shifts of β -1,3 *N*-acetyl-glucosamine pentasaccharide [53] supports this conclusion.

Summarizing these data, it can be concluded that polysaccharide B consists of a β -1,3-*N*-acetyl-*D*-glucosamine backbone with C4 either branched with C3-sulfated fucose (M1/M2) or sulfated (M3/M4). In M2, the C6 position of GlcNAc is sulfated. It is interesting to note that the H5 of fucose has high chemical shift (4.75 ppm) which indicates that fucose is stacked above the preceding GlcNAc residue in the manner seen in the fCS [40]. This is also supported by NOE cross peaks seen in the 2D ^1H , ^{13}C HSQC-NOESY spectrum between H5, H6 of fucose and H2 of GlcNAc. It is not possible to determine how these various structural motifs are distributed throughout polysaccharide B, but effects of neighboring residues are responsible for slight variation of chemical shifts e.g. M3 vs M4 and also H1/C1 of fucose, which enabled the presented structural analysis. These variations are likely caused by a different conformation adopted by a different primary structure as indicated by MD simulation (data not shown). Integration of isolated H5/C5 HSQC cross peaks allowed us to estimate the ratio of different GlcNAc types designated

M1:M2:M3:M4 at 22:27:27:24 %. Given the likely errors on these integrals, it is more appropriate to state that each occurs with equal probability.

3.5 *In vitro* biochemical characteristics of the sea squirt poly- and oligo- saccharides VRP327A and VRP327B

The biological activity (see section 3.6 for detailed description) and chemical composition of the sea squirt polysaccharides A and B are summarised in Table 4. Since, it was impossible to prepare pure samples, these data given are for the samples that contain both polysaccharides, but are enriched for one of the two. As mentioned above, VRP327A contains 83% polysaccharide A and 13% B, whereas VRP327B contains 20% polysaccharide A and 73% B. Both preparations were resistant to heparinase and chondroitinase ABC, likely because of the high sulfation of the DS contained in the sea squirt samples and non-GAG branched nature of polysaccharide B.

Table 3: Summary of the *in vitro* biological activity, and characteristics of a range of novel marine GAG-like polysaccharides.

ID	Dominant (80%) polysaccharide	XTT %	APTT IU/ml	NE %	MW (kDa)	Fucose molar %	GlcNAc molar %	GalNAc molar %	Sulfate %	N
VRP327 A	A	100	6.22	37.7	170	3.1	15.7	37.3	19.2	8
VRP327 B	B	91.4	4.2	36.9	115	21.9	45.8	14.1	17.5	2
VRP327 mixed	Mixed	90.1	4.4	45.9	86.9	11.9	25.8	23.0	16.7	4

VRP327A & B defined on the basis of monosaccharide composition, as confirmed by NMR. Data expressed as mean values from multiple different batches of polysaccharide (XTT, % viability relative to control; Neutrophil Elastase (NE) % activity compared with control).

Monosaccharide molar composition expressed as % of total monosaccharides. APTT represents mean values in IU/ml. N = number of samples

A. aspersa polysaccharides A & B have no appreciable cellular toxicity as cells treated with these polysaccharides demonstrated a viability of >90 %, using XTT as a metabolic viability indicator. The polysaccharides were shown to have < 10 IU/mg anticoagulant activity, as determined by the activated partial thromboplastin time (APTT) assay using human plasma (Table 4). Separate analysis (data not shown) of one sample of polysaccharide A identified low (<1 IU / mg) antithrombin mediated anti-Xa and anti-IIa activity, and low heparin cofactor II inhibition of thrombin, which were all comparable to mammalian DS.

Two polysaccharide samples were depolymerised using Fenton type free radical depolymerisation. The first sample was predominantly polysaccharide A (71% polysaccharide A, 20 % polysaccharide B). The second sample was mixed, containing almost equal percentages of polysaccharide A (43%) and polysaccharide B (48%). Oligosaccharides of various sizes were generated and tested for various biological activities *in vitro*. The degree of polymerisation (DP) of the fractions were nominally assigned based on the molecular weights of heparin oligosaccharide standards. The neutrophil elastase inhibition activity showed some correlation with chain length (Table 5). Cytotoxicity and anticoagulant activity of all depolymerised samples did not differ from that of the native polysaccharides (Table 5). The structure of the oligosaccharides produced from the mixed sample were analysed by NMR and it was found that they contained stronger signals attributable to a polysaccharide B like structure, rather than polysaccharide A structures (Figure 2). This indicated that the DS component of the sea squirt samples was preferentially depolymerised by the free

radical depolymerisation, probably through destruction of the IdoA monosaccharides and the opening of the GalNAc rings [54].

Table 4: The effect of various oligosaccharides on inhibition of neutrophil elastase expressed as % activity of each oligosaccharide compared with control (polysaccharide).

Nominal DP	Polysaccharide A NE %	XTT %	APTT IU/ml	Mixed polysaccharide NE %	XTT %	APTT IU/ml
Polysaccharide	38.95	96	ND	55.56	105	4.34
Dp2	NA	NA	NA	129.58	ND	ND
Dp4	68.1	121	1.56	100.65	ND	ND
Dp8	66.5	130	1.95	72.71	ND	ND
Dp12	57.6	117	2.56	41.67	ND	ND
Dp16	48.7	103	2.83	62.42	ND	ND
Dp20	57.3	100	2.83	NA	NA	NA

ND – Not determined. NA – Not applicable. DP – degree of polymerisation.

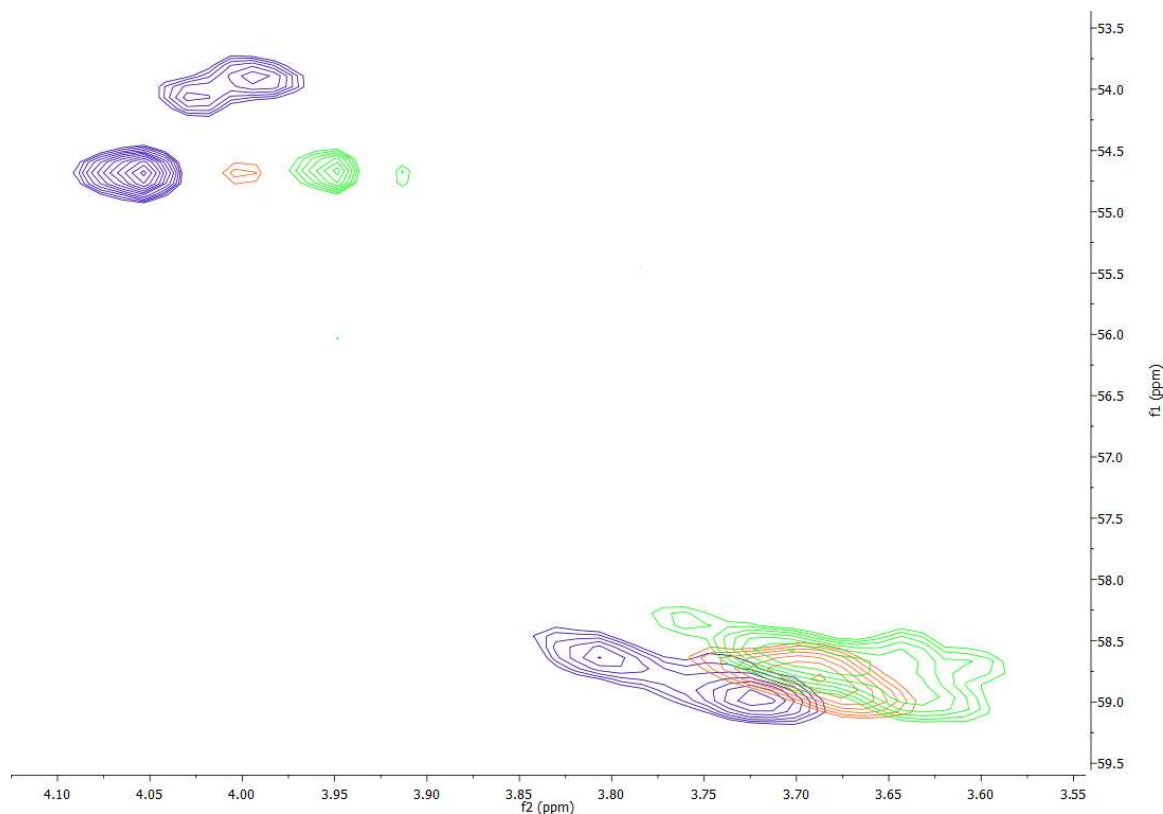


Figure 2: Superposition of the H2/C2 region of the 2D ^1H , ^{13}C HSQC spectra of the mixture of polysaccharides A and B (blue), polysaccharide B rich sample (red) and the oligosaccharides derived from polysaccharides A and B mixture (green). The signals in the top left corner belong to GalNAc of polysaccharide A, whereas the signals in the bottom right corner belong to GlcNAc of polysaccharide B. The red and green cross peaks have been moved by 0.05 and 0.1 ppm to the right, respectively, in order for their intensity to be clearly visible.

3.6 *In vitro* anti-inflammatory activity of sea squirt polysaccharides and oligosaccharides.

The anti-inflammatory activity of the sea squirt polysaccharides was demonstrated by measuring their effect on the release of elastase from human neutrophils and adhesion of human neutrophils to human umbilical cord endothelial cells (Figure 3). The inhibition of neutrophil elastase release is summarised in Table 4 above. Human neutrophils treated with polysaccharide A (VRP327A), polysaccharide B (VRP327B) or fucoidan (a reference polysaccharide isolated from *Fucus vesiculosus*) inhibited elastase release by 60-80 % (Figure 3a). Transendothelial migration of neutrophils

was inhibited by up to 30%, which did not reach significance (Figure 3c). Similarly, many of the VRP327 oligosaccharides also inhibited neutrophil elastase release (Figure 3c). However, there was no significant effect on neutrophil adhesion with any of the VRP327 oligosaccharides (Figure 3b).

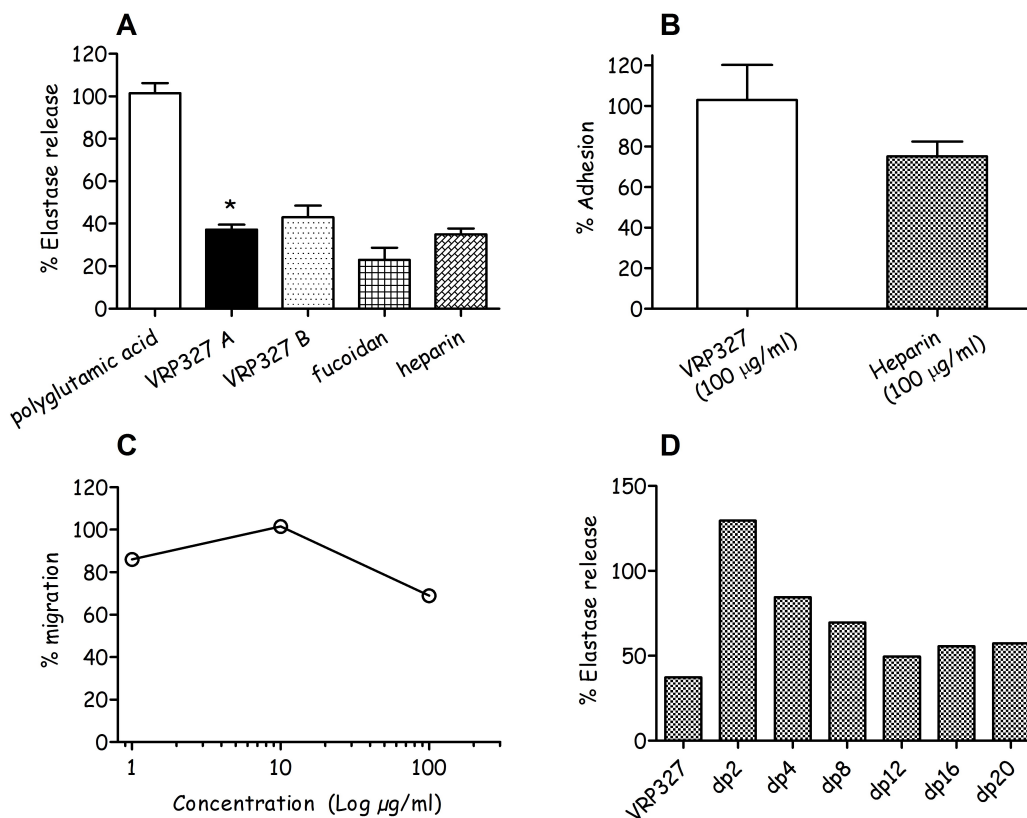


Figure 3: A,D) Percentage of elastase release from human neutrophils by the sea squirt polysaccharides and oligosaccharides (100 µg/ml). Each column represents mean + SEM from N (left to right; 19, 8, 4, 46, 19 respectively) separate donors performed in duplicate. * $P < 0.05$ compared with polyglutamic acid control. B) The effect of the heparin on human neutrophil adhesion and C) VRP327 on transmigration of human neutrophils in vitro. The results indicate that there is no significant reduction of adhesion of human neutrophils to human umbilical cord vein endothelial cells. In contrast, migration of human neutrophils through endothelial cells appeared to be inhibited.

3.4 *In vivo* anti-inflammatory activity of sea squirt polysaccharide A and oligosaccharides.

The inflammatory stimulus, zymosan caused a neutrophil rich infiltrate 4 h after injection into the peritoneal cavity, with neutrophils representing 75 % of the total cell

population. The administration of the polysaccharide A VRP327A by the intravenous route, 15 min prior to the intraperitoneal injection of zymosan, dose-dependently inhibited this response. Animals exposed to VRP327A (0.1-10 mg/kg) produced a dose-dependent inhibition of neutrophil recruitment to the peritoneal cavity in response to zymosan (Figure 4A). Fucoidan derived from *F. vesiculosus* (Figure 4B) at doses of 1 -100 mg/kg was used as a positive control and also caused a dose-dependent inhibition of neutrophil recruitment into the peritoneal cavity after challenge with zymosan. VRP327 oligosaccharides were further evaluated for their *in vivo* anti-inflammatory activity. Dp4, dp12 and dp16 demonstrated anti-inflammatory activity, whilst dp8 and dp20 were less effective against neutrophil recruitment (Figure 4 C,D).

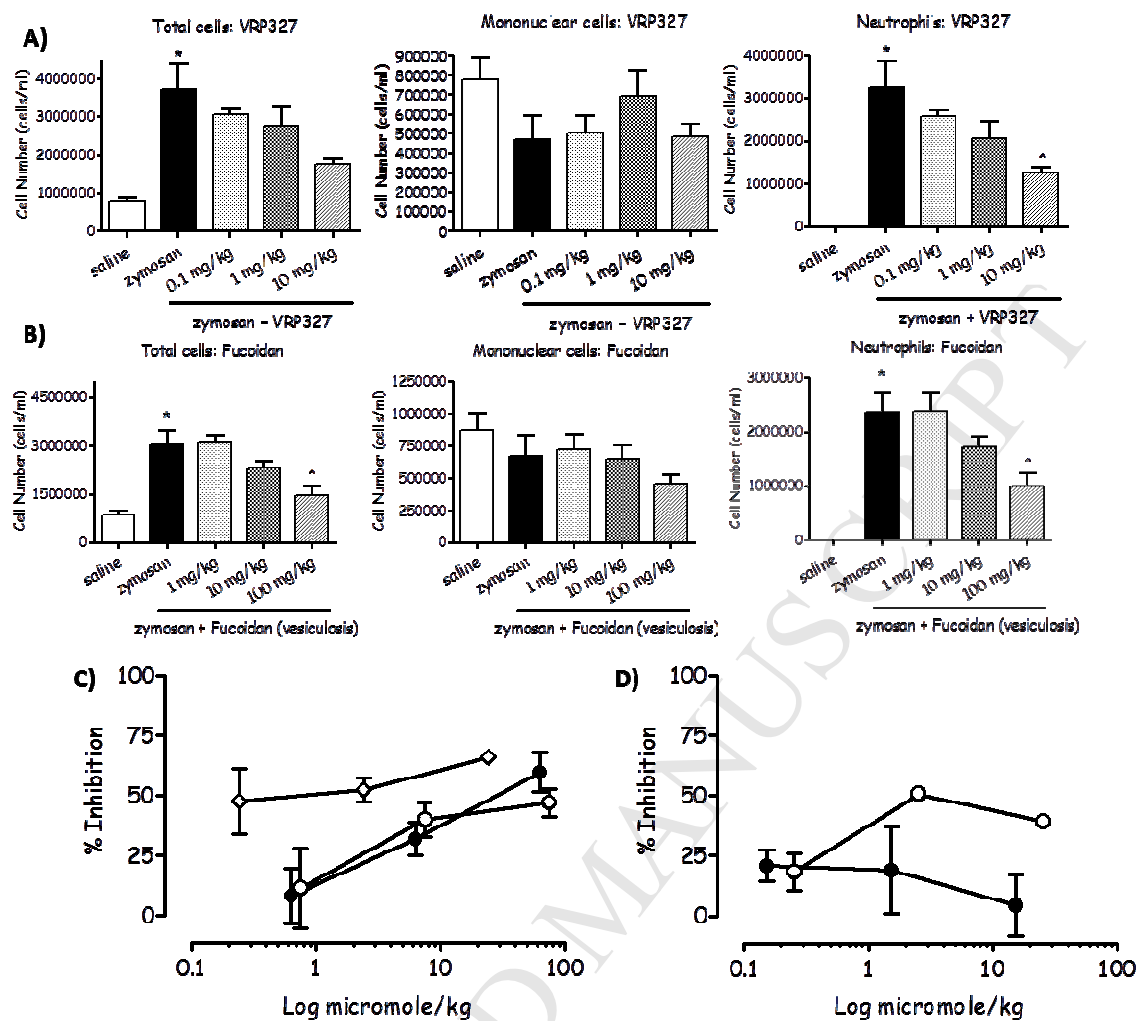


Figure 4: Inhibition of neutrophil recruitment to the peritoneal cavity. Animals were pretreated intravenously with saline (zymosan only treated group), VPR327 (A) and a fucosylated fucoidan control (B) 15 min prior to zymosan injection. Each column represents the mean cell number from 3-5 animals and vertical lines represent standard error of the mean. * $P < 0.01$ versus saline. ^ $P < 0.05$ of zymosan only (Dunnett's post hoc test). C) Inhibitory cumulative dose response curves for dp4 (closed circles), dp8 (open circles) and dp16 (open diamonds) and D) dp12 (open circles) and dp20 (closed circles) (B) against neutrophil recruitment to the peritoneal cavity induced by zymosan. The dose of VPR327 series was expressed as micromole/kg. The dependent variable (% Inhibition = $100 - \% \text{ control}$) was calculated by normalizing neutrophil cell number in drug treated animals by the mean neutrophil cell number in untreated animals. Each point is the mean \pm standard error of the mean of 3 animals.

4. Conclusions

A mixture of sulfated polysaccharides referred to as VPR327 was isolated from the gut of the tunicate *A. aspersa*. The two major polysaccharides (A and B; VPR327A and VPR327B) were fully characterised structurally by NMR. . The first of

these polysaccharides, polysaccharide A (VRP327A), is a highly sulfated dermatan sulfate, which contains unsulfated uronic acid and GalNAc of different sulfation patterns, with GalNAc 4,6S being the main component. The second polysaccharide (VRP327B) is a fucosylated sulfated molecule, containing a repeating monosaccharide unit of β -1,3-N-acetyl-D-glucosamine, approximately half of which are fucosylated on C4. These polysaccharides are interesting because they show anti-inflammatory properties, but importantly lack significant anticoagulant activity and direct cytotoxicity towards mammalian cells.

Both were shown to have anti-inflammatory activity *in vitro* and *in vivo*, while their anti-coagulant activity was low. Fractionation of VRP327 yielded oligosaccharides, which exhibited varying degrees of anti-inflammatory activity *in vivo* in the zymosan-induced neutrophilia assay. In particular dp4, dp12 and dp16 resulted in a dose dependent reduction in zymosan-induced neutrophilia in the peritoneal cavity. The fact that these oligosaccharides lack significant anticoagulant activities raises the possibility of using them as low molecular weight templates in the search for novel anti-inflammatory drugs.

Though HPLC separation was unable to distinguish the two polysaccharide components of VRP327, the NMR signals of the two polysaccharides are distinct. Polysaccharide A is a dermatan sulfate with an unusual sulfation pattern and contains disulfated GalNAc 4,6 SO₃, which has only been found in traces in previous Ascidian preparations (<1%) [27]. However, even more unique is the second polysaccharide isolated from *A. Aspersa*, which has been identified as a fucosylated chitin-like molecule. Whereas chitin is formed by a $1\beta \rightarrow 4$ linkage between its GlcNAc monomers, the GlcNAc polymer we isolated is comprised by GlcNAc linked with 1β

→ 3 linkage. It is also the first time that a fucosylated chitin-like polysaccharide is reported; previously fucosylated chitins identified being exclusively oligosaccharide moieties of glycoproteins. Finally both GlcNAc and fucose of polysaccharide B are sulfated and this polysaccharide, like other sulfated chitins [55], exhibits some anticoagulant activity.

This observation is important because it further suggests that the anti-inflammatory activities of polysaccharides are independent of anticoagulant activities, supporting other work with heparin like molecules [11]. Previous studies have demonstrated inhibition of neutrophil elastase by a wide range of GAG's [45, 56] and sulfated polysaccharide from seaweeds, such as fucoidan [6].

Our initial assumption was that sulfation is required for the anti-inflammatory activity of the polysaccharides as has been described for other studies investigating the anti-proliferative and anti-secretory activity of GAGs [57]. However, further study of the extracts is required to fully characterise the anti-inflammatory properties of these novel molecules we have identified and in particular the role of sulfation. Nonetheless, this study clearly demonstrates that anti-inflammatory activity is present in polysaccharides with a very wide molecular weight range, including some of the small oligosaccharide derivatives of VRP327. Our results further support the concept that oligosaccharides from marine sources could provide a useful source of novel anti-inflammatory molecules lacking anticoagulant activity for the treatment of diseases such as asthma and COPD.

References

1. Molinski, T.F., Dalisay, D.S., Lievens, S.L., and Saludes, J.P. (2009). Drug development from marine natural products. *Nat Rev Drug Discov* 8, 69-85.
2. Borsig, L., Wang, L., Cavalcante, M.C., Cardilo-Reis, L., Ferreira, P.L., Mourao, P.A., Esko, J.D., and Pavao, M.S. (2007). Selectin blocking activity of a fucosylated chondroitin sulfate glycosaminoglycan from sea cucumber. Effect on tumor metastasis and neutrophil recruitment. *J Biol Chem* 282, 14984-14991.
3. Volpi, N., and Maccari, F. (2009). Structural characterization and antithrombin activity of dermatan sulfate purified from marine clam *Scapharca inaequalvis*. *Glycobiology* 19, 356-367.
4. Belmiro, C.L., Castelo-Branco, M.T., Melim, L.M., Schanaider, A., Elia, C., Madi, K., Pavao, M.S., and de Souza, H.S. (2009). Unfractionated heparin and new heparin analogues from ascidians (chordate-tunicate) ameliorate colitis in rats. *J Biol Chem* 284, 11267-11278.
5. Brito, A.S., Arimateia, D.S., Souza, L.R., Lima, M.A., Santos, V.O., Medeiros, V.P., Ferreira, P.A., Silva, R.A., Ferreira, C.V., Justo, G.Z., et al. (2008). Anti-inflammatory properties of a heparin-like glycosaminoglycan with reduced anti-coagulant activity isolated from a marine shrimp. *Bioorg Med Chem* 16, 9588-9595.
6. Cumashi, A., Ushakova, N.A., Preobrazhenskaya, M.E., D'Incecco, A., Piccoli, A., Totani, L., Tinari, N., Morozevich, G.E., Berman, A.E., Bilan, M.I., et al. (2007). A comparative study of the anti-inflammatory, anticoagulant, antiangiogenic, and antiadhesive activities of nine different fucoidans from brown seaweeds. *Glycobiology* 17, 541-552.
7. Bavington, C.D., Lever, R., Mulloy, B., Grundy, M.M., Page, C.P., Richardson, N.V., and McKenzie, J.D. (2004). Anti-adhesive glycoproteins in echinoderm mucus secretions. *Comp Biochem Physiol B Biochem Mol Biol* 139, 607-617.
8. Page, C.P. (2001). One explanation of the asthma paradox: inhibition of natural anti-inflammatory mechanism by beta 2-agonists. *Lancet* 337, 717-720.
9. Fryer, A., Huang, Y.C., Rao, G., Jacoby, D., Mancilla, E., Whorton, R., Piantadosi, C.A., Kennedy, T., and Hoidal, J. (1997). Selective O-desulfation produces nonanticoagulant heparin that retains pharmacological activity in the lung. *J Pharmacol Exp Ther* 282, 208-219.
10. Seeds, E.A., and Page, C.P. (2001). Heparin inhibits allergen-induced eosinophil infiltration into guinea-pig lung via a mechanism unrelated to its anticoagulant activity. *Pulm Pharmacol Ther* 14, 111-119.
11. Lever, R., and Page, C.P. (2012). Non-anticoagulant effects of heparin: an overview. *Handb Exp Pharmacol*, 281-305.
12. Roy, S., Lai, H., Zouaoui, R., Duffner, J., Zhou, H., L, P.J., Zhao, G., Ganguly, T., Kishimoto, T.K., and Venkataraman, G. (2011). Bioactivity screening of partially desulfated low-molecular-weight heparins: a structure/activity relationship study. *Glycobiology* 21, 1194-1205.

13. Zhang, S., Condac, E., Qiu, H., Jiang, J., Gutierrez-Sanchez, G., Bergmann, C., Handel, T., and Wang, L. (2012). Heparin-induced leukocytosis requires 6-O-sulfation and is caused by blockade of selectin- and CXCL12 protein-mediated leukocyte trafficking in mice. *J Biol Chem* 287, 5542-5553.
14. Shodai, T., Suzuki, J., Kudo, S., Itoh, S., Terada, M., Fujita, S., Shimazu, H., and Tsuji, T. (2003). Inhibition of P-selectin-mediated cell adhesion by a sulfated derivative of sialic acid. *Biochem Biophys Res Commun* 312, 787-793.
15. Lever, R., and Page, C.P. (2002). Novel drug development opportunities for heparin. *Nat Rev Drug Discov* 1, 140-148.
16. van Ophoven, A., Heinecke, A., and Hertle, L. (2005). Safety and efficacy of concurrent application of oral pentosan polysulfate and subcutaneous low-dose heparin for patients with interstitial cystitis. *Urology* 66, 707-711.
17. Brown, R.A., Allegra, L., Matera, M.G., Page, C.P., and Cazzola, M. (2006). Additional clinical benefit of enoxaparin in COPD patients receiving salmeterol and fluticasone propionate in combination. *Pulm Pharmacol Ther* 19, 419-424.
18. Diamant, Z., Timmers, M.C., van, d.V., Page, C.P., van der Meer, F.J., and Sterk, P.J. (1996). Effect of inhaled heparin on allergen-induced early and late asthmatic responses in patients with atopic asthma. *Am J Respir Crit Care Med* 153, 1790-1795.
19. Vancheri, C., Mastruzzo, C., Armato, F., Tomaselli, V., Magri, S., Pistorio, M.P., LaMicela, M., D'Amico, L., and Crimi, N. (2001). Intranasal heparin reduces eosinophil recruitment after nasal allergen challenge in patients with allergic rhinitis. *J Allergy Clin Immunol* 108, 703-708.
20. Bendstrup, K.E., Gram, J., and Jensen, J.I. (2002). Effect of inhaled heparin on lung function and coagulation in healthy volunteers. *Eur Respir J* 19, 606-610.
21. Duong, M., Cockcroft, D., Boulet, L.P., Ahmed, T., Iverson, H., Atkinson, D.C., Stahl, E.G., Watson, R., Davis, B., Milot, J., et al. (2008). The effect of IVX-0142, a heparin-derived hypersulfated disaccharide, on the allergic airway responses in asthma. *Allergy* 63, 1195-1201.
22. Groth, I., Grunewald, N., and Alban, S. (2009). Pharmacological profiles of animal- and nonanimal-derived sulfated polysaccharides--comparison of unfractionated heparin, the semisynthetic glucan sulfate PS3, and the sulfated polysaccharide fraction isolated from *Delesseria sanguinea*. *Glycobiology* 19, 408-417.
23. Klajnert, B., Cortijo-Arellano, M., Bryszewska, M., and Cladera, J. (2006). Influence of heparin and dendrimers on the aggregation of two amyloid peptides related to Alzheimer's and prion diseases. *Biochem Biophys Res Commun* 339, 577-582.
24. Volpi, N. (2010). Dermatan sulfate: Recent structural and activity data. *Carbohydrate Polymers* 82, 233-239.
25. Fernandez, F., Vanryn, J., Ofosu, F.A., Hirsh, J., and Buchanan, M.R. (1986). The hemorrhagic and antithrombotic effects of dermatan sulfate. *British Journal of Haematology* 64, 309-317.
26. Pavão, M.S., Mourão, P.A., Mulloy, B., and Tollefsen, D.M. (1995). A unique dermatan sulfate-like glycosaminoglycan from ascidian. Its structure and the effect of its unusual sulfation pattern on anticoagulant activity. *J Biol Chem* 270, 31027-31036.

27. Pavao, M.S.G., Aiello, K.R.M., Werneck, C.C., Silva, L.C.F., Valente, A.P., Mulloy, B., Colwell, N.S., Tollefsen, D.M., and Mourao, P.A.S. (1998). Highly sulfated dermatan sulfates from ascidians - Structure versus anticoagulant activity of these glycosaminoglycans. *Journal of Biological Chemistry* *273*, 27848-27857.
28. Souza, C.P., Almeida, B.C., Colwell, R.R., and Rivera, I.N. (2011). The Importance of Chitin in the Marine Environment. *Mar Biotechnol* (NY).
29. Quinto, C., Wijffjes, A.H.M., Bloemberg, G.V., BlokTip, L., LopezLara, I.M., Lugtenberg, B.J.J., ThomasOates, J.E., and Spaink, H.P. (1997). Bacterial nodulation protein NodZ is a chitin oligosaccharide fucosyltransferase which can also recognize related substrates of animal origin. *Proceedings of the National Academy of Sciences of the United States of America* *94*, 4336-4341.
30. López-Lara, I.M., Blok-Tip, L., Quinto, C., Garcia, M.L., Stacey, G., Bloemberg, G.V., Lamers, G.E., Lugtenberg, B.J., Thomas-Oates, J.E., and Spaink, H.P. (1996). NodZ of *Bradyrhizobium* extends the nodulation host range of *Rhizobium* by adding a fucosyl residue to nodulation signals. *Mol Microbiol* *21*, 397-408.
31. Park, S.Y., Lee, S.H., Kawasaki, N., Itoh, S., Kang, K., Ryu, S.H., Hashii, N., Kim, J.M., Kim, J.Y., and Kim, J.H. (2011). α 1-3/4 fucosylation at Asn 241 of β -haptoglobin is a novel marker for colon cancer: a combinatorial approach for development of glycan biomarkers. *Int J Cancer*.
32. Oriol, R., Mollicone, R., Cailleau, A., Balanzino, L., and Breton, C. (1999). Divergent evolution of fucosyltransferase genes from vertebrates, invertebrates, and bacteria. *Glycobiology* *9*, 323-334.
33. Staudacher, E., Altmann, F., Wilson, I.B.H., and Marz, L. (1999). Fucose in N-glycans: from plant to man. *Biochimica Et Biophysica Acta-General Subjects* *1473*, 216-236.
34. Miyoshi, E., Noda, K., Yamaguchi, Y., Inoue, S., Ikeda, Y., Wang, W.G., Ko, J.H., Uozumi, N., Li, W., and Taniguchi, N. (1999). The alpha 1-6-fucosyltransferase gene and its biological significance. *Biochimica Et Biophysica Acta-General Subjects* *1473*, 9-20.
35. Taniguchi, N., Miyoshi, E., Gu, J., Honke, K., and Matsumoto, A. (2006). Decoding sugar functions by identifying target glycoproteins. *Current Opinion in Structural Biology* *16*, 561-566.
36. Volpi, N., Mascellani, G., and Bianchini, P. (1992). Low molecular weight heparins (5 kDa) and oligoheparins (2 kDa) produced by gel permeation enrichment or radical process: comparison of structures and physicochemical and biological properties. *Anal Biochem* *200*, 100-107.
37. Bitter, T., and Muir, H.M. (1962). A modified uronic acid carbazole reaction. *Anal Biochem* *4*, 330-334.
38. Terho, T.T., and Hartiala, K. (1971). Method for determination of the sulfate content of glycosaminoglycans. *Anal Biochem* *41*, 471-476.
39. Skidmore, M.A., Guimond, S.E., Dumax-Vorzet, A.F., Atrih, A., Yates, E.A., and Turnbull, J.E. (2006). High sensitivity separation and detection of heparan sulfate disaccharides. *J Chromatogr A* *1135*, 52-56.
40. Panagos, C., Thomson, D.S., Moss, C., Hughes, A.D., Kelly, M.S., Liu, Y., Chai, W., Venkatasamy, R., Spina, D., Page, C.P., et al. (2014). Fucosylated chondroitin sulfates from the body wall of the sea cucumber *Holothuria forskali*. Conformation, selectin binding and biological activity. *J Biol Chem*.

41. Vandergraaf, F., Keus, F.J.A., Vlooswijk, R.A.A., and Bouma, B.N. (1982). The contact activation mechanism in human plasma - activation induced by dextran sulfate. *Blood* 59, 1225-1233.
42. Lever, R., Haq, S., Grundy, M.M., Richardson, N.V., and Page, C.P. (1999). Effects of heparinases and heparin upon the adhesive functions and surface characteristics of human umbilical; Vein endothelial cells. *British Journal of Pharmacology* 126, U27-U27.
43. Smailbegovic, A., Lever, R., and Page, C.P. (2001). The effects of heparin on the adhesion of human peripheral blood mononuclear cells to human stimulated umbilical vein endothelial cells. *British Journal of Pharmacology* 134, 827-836.
44. Brown, R.A., Lever, R., Jones, N.A., and Page, C.P. (2003). Effects of heparin and related molecules upon neutrophil aggregation and elastase release in vitro. *British Journal of Pharmacology* 139.
45. Lever, R., Lo, W.T., Faraidoun, M., Amin, V., Brown, R.A., Gallagher, J., and Page, C.P. (2007). Size-fractionated heparins have differential effects on human neutrophil function in vitro. *British Journal of Pharmacology* 151, 837-843.
46. Lever, R., Smailbegovic, A., and Page, C.P. (2010). Locally available heparin modulates inflammatory cell recruitment in a manner independent of anticoagulant activity. *European Journal of Pharmacology* 630, 137-144.
47. Moffatt, J.D., Lever, R., and Page, C.P. (2004). Effects of inhaled thrombin receptor agonists in mice. *Br.J.Pharmacol* 143, 269-275.
48. Guerrini, M., Beccati, D., Shriver, Z., Naggi, A., Viswanathan, K., Bisio, A., Capila, I., Lansing, J.C., Guglieri, S., Fraser, B., et al. (2008). Oversulfated chondroitin sulfate is a contaminant in heparin associated with adverse clinical events. *Nat Biotechnol* 26, 669-675.
49. Sanderson, P.N., Huckerby, T.N., and Nieduszynski, I.A. (1989). Chondroitinase ABC digestion of dermatan sulphate. N.m.r. spectroscopic characterization of the oligo- and poly-saccharides. *Biochem J* 257, 347-354.
50. Bossennec, V., Petitou, M., and Perly, B. (1990). H-1-NMR investigation of naturally occurring and chemically oversulphated dermatan sulphates - identification of minor monosaccharide residues. *Biochemical Journal* 267.
51. Huckerby, T.N., Lauder, R.M., Brown, G.M., Nieduszynski, I.A., Anderson, K., Boocock, J., Sandall, P.L., and Weeks, S.D. (2001). Characterization of oligosaccharides from the chondroitin sulfates. (1)H-NMR and (13)C-NMR studies of reduced disaccharides and tetrasaccharides. *Eur J Biochem* 268, 1181-1189.
52. Yates, E.A., Santini, F., Guerrini, M., Naggi, A., Torri, G., and Casu, B. (1996). H-1 and C-13 NMR spectral assignments of the major sequences of twelve systematically modified heparin derivatives. *Carbohydrate Research* 294, 15-27.
53. Morando, M., Yao, Y., Martin-Santamaria, S., Zhu, Z., Xu, T., Canada, F.J., Zhang, Y., and Jimenez-Barbero, J. (2010). Mimicking chitin: chemical synthesis, conformational analysis, and molecular recognition of the beta(1->3) N-acetylchitopentaose analogue. *Chemistry* 16, 4239-4249.
54. Panagos, C., Thomson, D., Bavington, C.D., and Uhrin, D. (2012). Structural characterisation of oligosaccharides obtained by Fenton-type radical depolymerisation of dermatan sulfate. *Carbohydrate Polymers* 87, 2086-2092.

55. Jayakumar, R., Nwe, N., Tokura, S., and Tamura, H. (2007). Sulfated chitin and chitosan as novel biomaterials. *Int J Biol Macromol* *40*, 175-181.
56. Lever, R., Lo, W.T., Brown, R.A., Gallagher, J., and Page, C.P. (2003). The effects of heparin fractions of defined chain length on human neutrophil functions in vitro. *British Journal of Pharmacology* *140*.
57. Kanabar, V., Page, C., Simcock, D.E., Karner, C., Mahn, K., O'Connor, B.J., and Hirst, S.J. (2008). Heparin and structurally related polymers attenuate eotaxin-1 (CCL11) release from human airway smooth muscle. *British Journal of Pharmacology* *154*, 833-842.

ACCEPTED MANUSCRIPT